Geophys. J. R. astr. Soc. (1983) **75**, 669–691

Calculation of the elasto-dynamic Green's function in layered media by means of a modified propagator matrix method

Ghislain R. Franssens *University of Gent, Laboratorium voor Electromagnetisme en Acustica, Sint-Pietersnieuwstraat 41, B-9000 Gent, Belgium*

Received 1983 March 29; in original form 1982 May 6

Summary. The calculation of the two-dimensional elasto-dynamic Green's function for a stratified medium is investigated. The solution is represented in the form of an inverse Fourier integral which is to be integrated along a properly chosen path in the complex wavenumber plane. The integrand is computed using a modified propagator matrix method.

This method is based on a mixed formulation using the propagator matrix and the matrix of minors of the propagator matrix (compound matrix). The major advantages of this approach are the elimination of the numerical loss of precision problems associated with the Thomson-Haskell formulation, without losing the attractive tractability and compactness of the propagator matrix method. This modified method is first mathematically derived, and theoretical seismograms are then presented for two examples.

1 Introduction

The computation of the two-dimensional Green's function in an isotropic, layered, elastic space is investigated. It is assumed that the elastic parameters vary stepwise and only in one direction (z-axis). The calculation of the elastic wave propagation in such a structure is a classic problem that has been treated by so many authors that it is impossible to give an exhaustive list here. During the past, several solution methods for this problem have been published. One of the first systematic approaches was introduced by Thomson (1950) and corrected by Haskell (1953). They developed transfer matrix methods which relate displacements and stresses at the top and bottom of the uniform layers. Later on, Haskell (1964) and Harkrider (1964) considered the excitation of Love and Rayleigh waves by realistic sources. Computational difficulties arise when these transfer matrix methods are applied for layer thicknesses which are large compared to the wavelength. In each layer, up- and downward propagating waves cause growing and decaying exponentials whereby the former must cancel in the final expressions. In finite accuracy calculations, this cancellation is not complete since the growing terms swamp the significant parts. To avoid that difficulty, a reformulation of the former method has been presented by Knopoff (1964) based on Laplace's development by minors. Other authors (Molotkov 1961; Dunkin 1965) involved higher order minors of the original matrices. A more systematic formulation of the transfer

matrix methods for a general stratification in elastic parameters has been given by Gilbert & Backus (1965). They also established the general utility of the compound matrix.

However, these formulations are still not satisfactory for high frequencies if applied to the calculation of the dispersion function, as recently pointed out by Abo-Zena (1979). In his paper, the author calculates the dispersion function by separating all frequency factors of the propagator matrix, thereby also avoiding the loss of significant digits. A completely different approach was introduced by Kennett & Kerry (1979) in which the response to a general source was presented in terms of the reflection and transmission properties of the regions above and below the source. More recently, a number of efficient and stable methods for performing seismic calculations related to the present work can be found in Woodhouse (1981).

In this paper, the time response due to a force line source with arbitrary location in a multilayered medium is presented (i.e. the elasto-dynamic Green's function). The displacement-stress field is written in the form of an inverse Fourier integral which is integrated along a properly chosen path in the complex wavenumber plane. A hybrid formulation in terms of propagator matrices and the compound matrices of the propagator matrices is used to calculate the integrand. This modified propagator matrix method avoids completely the numerical problem mentioned before. This means that very thick layers, which could not be analysed by the propagator matrix method, are now easily handled by the modified method. In the next section the classical propagator matrix formalism is briefly explained and the numerical problems associated with this method are emphasized. The modified propagator matrix method is presented in the third section. In the fourth section the integration method, used for the inverse Fourier integral, is described.

Finally, theoretical seismograms are presented for two examples, one being a simple model for the Borrego mountain earthquake event.

2 The propagator matrix method

Consider a multilayered, elastic space consiting of n layers sandwiched between two semi-infinite spaces as shown in Fig. 1. Each material is assumed to be isotropic, homogeneous, loss-free and perfectly elastic and can therefore be characterized by its density ρ_l and wave velocities v_{sl} and v_{pl}, $l = 0, 1, \ldots n+1$. Let u_i be the components of the displacement vector

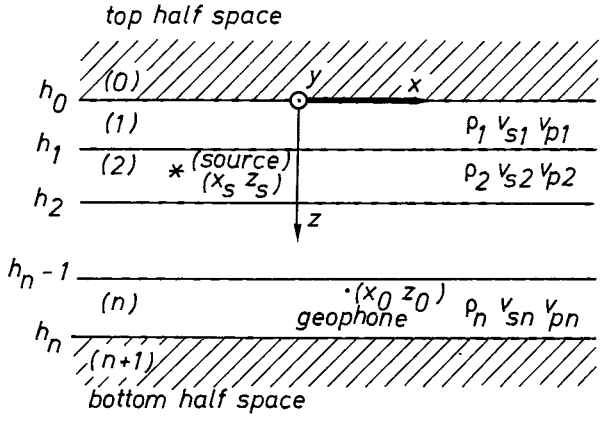

Figure 1. The investigated stratification: a stack of n homogeneous layers is terminated on each end with a semi-infinite space or a surface boundary condition.

and T_{ij} the stress tensor of the two-dimensional Green's function ($i, j = 1, 2, 3$). In each material they satisfy the linearized equations of motion given by, using Einstein's summation convection (see, for example, Aki & Richards 1980):

$$\partial_j T_{ij} - \rho \partial_t^2 u_i = s_i(t)\, \delta(x - x_s)\, \delta(z - z_s). \tag{2.1}$$

Herein are (x_s, z_s) the coordinates of a line source, with a time-dependent displacement amplitude $s_i(t)$ for the ith component. By $\partial_j, j = 1, 2, 3$ we denote the partial derivative with respect to x, y, z respectively. The stresses are related to the displacements by the constitutive equations:

$$T_{ij} = \tfrac{1}{2} C_{ijpq} (\partial_q u_p + \partial_p u_q), \qquad (i, j, p, q = 1, 2, 3), \tag{2.2}$$

with C_{ijpq} being the stiffness tensor for isotropic media. All materials are assumed to be in perfect elastic contact with each other (welded contact). This means that the displacement and the normal tractions are continuous over the layers interfaces:

$$\begin{aligned} &\lim_{z \lesssim h_l} u_i = \lim_{z \gtrsim h_l} u_i \qquad l = 0, 1, \ldots n \\ &\lim_{z \lesssim h_l} T_{i3} = \lim_{z \gtrsim h_l} T_{i3} \qquad i = 1, 2, 3. \end{aligned} \tag{2.3}$$

Finally, u_i and T_{ij} satisfy the radiation condition at infinity. For notational simplicity it is convenient to define displacement-stress vectors as follows (Gilbert & Backus 1965):

for *P–SV*-waves:

$$B(x, z, t) = [u_1 u_3 T_{13} T_{33}]^{\mathrm{T}}, \tag{2.4a}$$

for *SH*-waves:

$$B(x, z, t) = [u_2 T_{23}]^{\mathrm{T}}, \tag{2.4b}$$

where T stands for the transpose.

Let $\hat{B}(k, z, f)$ denote the two-dimensional Fourier transform of $B(x, z, t)$ so that:

$$B(x, z, t) = \frac{1}{2\pi} \int_{-\infty}^{+\infty} \exp(-j2\pi f t) \int_{-\infty}^{+\infty} \hat{B}(k, z, f) \exp[+jk(x - x_s)]\, dk\, df, \tag{2.5}$$

where f stands for the frequency and k for the wavenumber along the x-axis.

Substitution of (2.5) in the differential equations (2.1)–(2.2) yields two uncoupled sets of first-order, ordinary differential equations of the form:

$$\partial_z \hat{B}(k, z, f) = A(k, z, f)\, \hat{B}(k, z, f) + \hat{S}(f)\, \delta(z - z_s). \tag{2.6}$$

The matrix A can be considered as the system matrix, and $\hat{S}$ as a source vector. For *SH*-waves, A is a (2 x 2) complex matrix and $\hat{S}$ is:

$$\hat{S}(f) = [0 \quad S_2(f)]^{\mathrm{T}}. \tag{2.7a}$$

For *P–SV*-waves, A is a (4 x 4) complex matrix and $\hat{S}$ is:

$$\hat{S}(f) = [0 \quad 0 \quad S_1(f) \quad S_3(f)]^{\mathrm{T}}. \tag{2.7b}$$

The functions $S_i(f)$, ($i = 1, 2, 3$) are the Fourier transforms with respect to time of the source time functions $s_i(t)$.

For the explicit expressions of the A matrices see Appendix A.

The boundary conditions (2.3) are transformed into:

$$\lim_{z \lesssim h_l} \hat{B} = \lim_{z \gtrsim h_l} \hat{B}, \qquad l = 0, 1, \ldots, n, \tag{2.8}$$

and $\hat{B}$ should also satisfy the radiation condition for $z \to \pm\infty$. Let us define the levels (*cf.* Fig. 1):

$$z_1 \triangleq \min(z_s, h_0)$$
$$z_2 \triangleq \max(z_s, h_n). \tag{2.9}$$

The radiation condition implies that, for $z < z_1$, only upward travelling waves (waves travelling in the negative z-direction) can exist, while for $z > z_2$ only downward travelling waves can occur. To relate the displacement-stress vector more directly to the elastic wavefield we use the transformation:

$$\hat{B}(k, z, f) = D(k, z, f)\, V(k, z, f), \tag{2.10}$$

following Kennett, Kerry & Woodhouse (1978). The matrix D is the eigenvector matrix of the system matrix A and has been introduced by Dunkin (1965). The elements of the vector V, called the wavevector, can be identified with the amplitudes of upward and downward travelling planewaves:

$$V = [V_U \; V_D]^T, \tag{2.11}$$

(V_U, V_D: scalars for *SH*-waves, (1×2) for *P–SV*-waves). According to the radiation condition, the wavevector at the level z_1 should have the form:

$$V(k, z_1, f) = [V_U(k, z_1, f) \qquad 0]^T, \tag{2.12a}$$

and at the level z_2:

$$V(k, z_2, f) = [0 \qquad V_D(k, z_2, f)]^T. \tag{2.12b}$$

Substituting (2.12a) and (2.12b) in (2.10) we obtain at $z = z_p$ $(p = 1, 2)$:

$$\hat{B}(k, z_p, f) = C(z_p)\, X_p \tag{2.13}$$

with:

$$C(z_p) = \begin{bmatrix} D_{1p} \\ D_{2p} \end{bmatrix} \tag{2.14}$$

and the column vectors X_p given by:

$$X_1 = V_U^T, \qquad X_2 = V_D^T. \tag{2.15}$$

Herein are D_{pq} $(p, q = 1, 2)$ subpartitions of the eigenvector matrix D.

Instead of having a semi-infinite space at $z = z_p$, we can also apply one of the following boundary conditions:

(i) a stress-free surface:

$$\text{with } C(z_p) = \begin{bmatrix} I \\ 0 \end{bmatrix} \text{ and } X_p = \begin{bmatrix} \hat{u}_1 \\ \hat{u}_3 \end{bmatrix} \qquad \text{on } z = z_p; \tag{2.16}$$

(ii) a rigid surface:

$$\text{with } C(z_p) = \begin{bmatrix} 0 \\ I \end{bmatrix} \text{ and } X_p = \begin{bmatrix} \hat{T}_{13} \\ \hat{T}_{33} \end{bmatrix} \qquad \text{on } z = z_p; \tag{2.17}$$

(iii) a loaded surface with mass load σ(kg m^{-2}):

$$\text{with } C(z_p) = \begin{bmatrix} I \\ \pm(2\pi f)^2 \end{bmatrix} \text{ and } X_p = \begin{bmatrix} \hat{u}_1 \\ \hat{u}_3 \end{bmatrix} \qquad \text{on } z = z_p, \tag{2.18}$$

where I is the unity matrix. In (2.18) holds the plus sign for $p = 2$, the minus sign for $p = 1$.

Our aim, stated so far, is to obtain a solution for the differential system (2.6) together with the boundary conditions (2.8) and (2.13). In the propagator matrix method this is done using a 'propagator matrix' $P(z, z')$ (Gilbert & Backus 1965) or 'matricant' (Gantmacher 1959) which is a fundamental matrix solution of the homogeneous differential system, with linear independent columns under the constraint $P(z, z) = I$. If $\Phi(z)$ is any fundamental matrix solution of the homogeneous system, the propagator matrix $P(z, z')$ can be derived from it as follows:

$$P(z, z') = \Phi(z)\,\Phi^{-1}(z'). \tag{2.19}$$

The name 'propagator matrix' comes from the fact that once $\hat{B}$ is known at some level z', it can be propagated toward another level z by a simple matrix multiplication:

$$\hat{B}(z) = P(z, z')\,\hat{B}(z'). \tag{2.20}$$

The general form of the propagator matrix is stated in Appendix B. The explicit expressions can be found elsewhere (e.g. Dunkin 1965).

The propagator matrix can also be used to find the solution of the inhomogeneous system by applying the formula:

$$\hat{B}(z) = P(z, z')\,\hat{B}(z') + \int_{z'}^{z} P(z, \zeta)\,\hat{S}\delta(\zeta - z_s)\,d\zeta. \tag{2.21}$$

For more details about the propagator matrix we refer, for example, to Gilbert & Backus (1965). We limit ourselves here to a brief enumeration of some useful characteristics of the propagator matrix:

$$\det[P(z, z')] = \exp\left\{\int_{z'}^{z} \operatorname{trace}[A(k, \zeta, f)]\,d\zeta\right\} = 1 \tag{2.22a}$$

$$P(z, z') = P(z', z)^{-1} \tag{2.22b}$$

$$P(z, z') = P(z, \zeta)\,P(\zeta, z') \qquad \zeta \in [z, z']. \tag{2.22c}$$

Furthermore, the propagator matrix over different layers is simply the product of the propagator matrices of each layer. This is due to the fact that the continuity of $\hat{B}$ ensures the continuity of $P(z, z')$. Therefore (2.21) is also valid through a stack of layers. Also from this expression it can be seen that $\hat{B}(z_s^-)$ and $\hat{B}(z_s^+)$, the displacement-stress vectors just before and after the source level z_s, make a jump by an amount $\hat{S}$:

$$\hat{B}(z_s^+) - \hat{B}(z_s^-) = \hat{S}. \tag{2.23}$$

In the case of a displacement source, as defined in (2.1), there is only a jump in the stress part of the $\hat{B}$ vector. Relating $\hat{B}(z_s^+)$ and $\hat{B}(z_s^-)$ to the displacement-stress vectors at $z = z_2$ and $z = z_1$ respectively, using (2.20) and combining this with (2.13), we obtain:

$$P(z_s, z_2)\, C(z_2)\, X_2 - P(z_s, z_1)\, C(z_1)\, X_1 = \hat{S}. \tag{2.24}$$

Numerical difficulties arise when one attempts to solve the above linear system of equations for layers thick compared to the wavelength. In the evanescent regime, that is for frequencies for which the sine functions in the propagator matrix become hyperbolic sine functions, one obtains exponentially growing terms (Kennett & Kerry 1979). It turns out that in numerical calculations those terms, which do not exist in the final result, do not cancel out exactly due to the round-off errors.

One way to avoid this difficulty is to calculate the determinants of (2.24) directly from the analytical expressions for the minors of the propagator matrix as suggested by Gilbert & Backus (1965) and demonstrated by Dunkin (1965).

In the following section we propose an alternative matrix formulation for the solution of (2.24), also based on that approach. However, this formulation still has the compactness of the propagator matrix method, without having its numerical problems and is therefore very well fitted to code on a computer.

3 The modified propagator matrix method

We consider again the system of linear equations (2.24):

$$P(z_s, z_2)\, C(z_2)\, X_2 - P(z_s, z_1)\, C(z_1)\, X_1 = \hat{S} \tag{3.1}$$

and define:

$$\begin{aligned} C(z_s^+) &\triangleq P(z_s, z_2)\, C(z_2) \\ C(z_s^-) &\triangleq P(z_s, z_1)\, C(z_1). \end{aligned} \tag{3.2}$$

Substitution of (3.2) in (3.1) yields:

$$\left[C(z_s^+)\ C(z_s^-)\right] \begin{bmatrix} X_2 \\ -X_1 \end{bmatrix} = \hat{S}. \tag{3.3}$$

The determinant Δ of the above matrix can be regarded as the determinant of the product of matrices:

$$\Delta \triangleq \det \left\{ \begin{bmatrix} I & I \end{bmatrix} \begin{bmatrix} C(z_s^+) & 0 \\ 0 & C(z_s^-) \end{bmatrix} \right\} \tag{3.4}$$

where I stands for the unity matrix of appropriate dimensions (4×4 for P–SV-waves, 2×2 for SH-waves). Using the Binet-Cauchy formula we can express the determinant Δ in terms of the minors of the rectangular matrices (Gantmacher 1959, p. 9).

If we define the following vectors of second-order minors (P–SV-waves):

$$\begin{aligned} \mathscr{C}(z_s^-) \triangleq \Bigg[& C(z_s^-) \begin{pmatrix} 1 & 2 \\ 1 & 2 \end{pmatrix}, C(z_s^-) \begin{pmatrix} 1 & 2 \\ 1 & 3 \end{pmatrix}, C(z_s^-) \begin{pmatrix} 1 & 2 \\ 1 & 4 \end{pmatrix}, \\ & C(z_s^-) \begin{pmatrix} 1 & 2 \\ 2 & 3 \end{pmatrix}, C(z_s^-) \begin{pmatrix} 1 & 2 \\ 2 & 4 \end{pmatrix}, C(z_s^-) \begin{pmatrix} 1 & 2 \\ 3 & 4 \end{pmatrix} \Bigg]^{\mathrm{T}} \end{aligned} \tag{3.5}$$

$$\mathscr{C}(z_s^+) \triangleq \left[C(z_s^+)\begin{pmatrix}1&2\\1&2\end{pmatrix}, C(z_s^+)\begin{pmatrix}1&2\\1&3\end{pmatrix}, C(z_s^+)\begin{pmatrix}1&2\\1&4\end{pmatrix},\right.$$
$$\left. C(z_s^+)\begin{pmatrix}1&2\\2&3\end{pmatrix}, C(z_s^+)\begin{pmatrix}1&2\\2&4\end{pmatrix}, C(z_s^+)\begin{pmatrix}1&2\\3&4\end{pmatrix}\right]^{\mathrm{T}} \tag{3.6}$$

the expression (3.4) can be put in matrix notation:

$$= \mathscr{C}^{\mathrm{T}}(z_s^+)\ \mathscr{I}_{00}\ \mathscr{C}(z_s^-) \tag{3.7}$$

with:

$$\mathscr{I}_{00} \triangleq \begin{bmatrix} 0 & 0 & 0 & 0 & 0 & 1 \\ 0 & 0 & 0 & 0 & -1 & 0 \\ 0 & 0 & 0 & 1 & 0 & 0 \\ 0 & 0 & 1 & 0 & 0 & 0 \\ 0 & -1 & 0 & 0 & 0 & 0 \\ 1 & 0 & 0 & 0 & 0 & 0 \end{bmatrix}. \tag{3.8a}$$

A similar result holds for *SH*-waves if we define:

$$\mathscr{C}(z_s^+) \triangleq C(z_s^+) \quad \text{and} \quad \mathscr{C}(z_s^-) \triangleq C(z_s^-)$$

with:

$$\mathscr{T}_{00} \triangleq \begin{bmatrix} 0 & 1 \\ -1 & 0 \end{bmatrix}. \tag{3.8b}$$

Returning to the *P–SV*-waves, we calculate the second-order compound matrix of the left hand side matrices in (3.2). Using the fact that the compound matrix of a product of matrices is the product of the compound matrices of those matrices (Gantmacher 1959 p. 21), we can write:

$$\mathscr{C}(z_s^+) = \mathscr{P}(z_s, z_2)\ \mathscr{C}(z_2) \tag{3.9}$$

$$\mathscr{C}(z_s^-) = \mathscr{P}(z_s, z_1)\ \mathscr{C}(z_1) \tag{3.10}$$

in which $\mathscr{C}(z_2)$ and $\mathscr{C}(z_1)$ are defined in an analogous way as in (3.5) and (3.6) together with (2.14). $\mathscr{P}(z_s, z_2)$ is the (6×6) second-order compound matrix of the propagator matrix $P(z_s, z_2)$, explicitly given in Appendix C. Since $P(z_s, z_2)$ is continuous across the layer boundaries, $\mathscr{P}(z_s, z_2)$ will also be continuous. Furthermore, just as an overall propagator matrix can be decomposed as the product of the propagator matrices of the individual layers, an overall compound matrix can be written as the product of the compound matrices of each layer. Substitution of (3.9) and (3.10) into (3.7) then yields:

$$\Delta = \mathscr{C}^{\mathrm{T}}(z_2)\ \mathscr{P}^{\mathrm{T}}(z_s, z_2)\ \mathscr{I}_{00}\ \mathscr{P}(z_s, z_1)\ \mathscr{C}(z_1) \tag{3.11}$$

For the *SH*-waves $\mathscr{P}(z, z')$ is identical with the propagator matrix $P(z, z')$.

By multiplication on the left of (3.3) with $P(z_s', z_s)$ it can be seen that the determinant Δ is independent of the source level z_s, since $\det[P(z_s', z_s)] = 1$.

Let us return to the system of equations (3.3) for P–SV-waves. First, we express the matrices $C(z_s^+)$ and $C(z_s^-)$ symbolic in terms of their elements as follows:

$$C(z_s^+) = (C_{ij}^+); C(z_s^-) = (C_{ij}^-), \qquad (i = 1, 4; j = 1, 2), \tag{3.12}$$

and:

$$\hat{S} = (\hat{s}_i), \quad (i = 1, 4). \tag{3.13}$$

Furthermore, it is useful to define the second-order compound matrices ($i = 1, 4$):

$$\mathscr{C}'(z_s^+) = \text{column vector of second-order minors of } [\hat{s}_i \; C_{i2}^+], \tag{3.14}$$

$$\mathscr{C}''(z_s^+) = \text{column vector of second-order minors of } [C_{i1}^+ \; \hat{s}_i] \tag{3.15}$$

in a similar way as in (3.6). Analogous definitions hold for $\mathscr{C}'(z_s^-)$ and $\mathscr{C}''(z_s^-)$.

The solution of the boundary system (3.1) can then be written in the form:

$$X_1 = -\frac{1}{\Delta}\begin{bmatrix} \mathscr{C}^{\mathrm{T}}(z_s^+)\; \mathscr{J}_{00}\, \mathscr{C}'(z_s^-) \\ \mathscr{C}^{\mathrm{T}}(z_s^+)\; \mathscr{J}_{00}\, \mathscr{C}''(z_s^-) \end{bmatrix} \quad X_2 = +\frac{1}{\Delta}\begin{bmatrix} \mathscr{C}^{\mathrm{T}}(z_s^-)\; \mathscr{J}_{00}^{\mathrm{T}}\, \mathscr{C}'(z_s^+) \\ \mathscr{C}^{\mathrm{T}}(z_s^-)\; \mathscr{J}_{00}^{\mathrm{T}}\, \mathscr{C}''(z_s^+) \end{bmatrix}. \tag{3.16}$$

The primed compound vectors are a linear combination of the components of the source vector $\hat{S}$. Thus:

$$\begin{aligned} &\mathscr{C}'(z_s^-) = \epsilon_-'\, \hat{S}; \quad \mathscr{C}'(z_s^+) = \epsilon_+'\, \hat{S} \\ &\mathscr{C}''(z_s^-) = -\epsilon_-''\, \hat{S}; \quad \mathscr{C}''(z_s^+) = -\epsilon_+''\, \hat{S} \end{aligned} \tag{3.17}$$

The dimensions of the ϵ-matrices are (6×4).

Now, suppose $z_1 \leqslant z_0 < z_s$. The displacement-stress vector $\hat{B}(z_0)$ at the observer level z_0 can be computed by propagating $\hat{B}(z_s^-)$ to z_0:

$$\hat{B}(z_0) = P(z_0, z_s)\, C(z_s^-)\, X_1 \triangleq C(z_0)\, X_1. \tag{3.18}$$

Substitution of (3.16) and (3.17) into (3.18) yields:

$$\hat{B}(z_0) = -\frac{1}{\Delta}\, C(z_0) \begin{bmatrix} \mathscr{C}^{\mathrm{T}}(z_s^+)\; \mathscr{J}_{00}\, \epsilon_-' \\ -\mathscr{C}^{\mathrm{T}}(z_s^+)\; \mathscr{J}_{00}\, \epsilon_-'' \end{bmatrix} \hat{S}. \tag{3.19}$$

In terms of the elements of the matrix $C(z_0)$ this becomes:

$$\hat{B}(z_0) = -\frac{1}{\Delta}\begin{bmatrix} \mathscr{C}^{\mathrm{T}}(z_s^+)\; \mathscr{J}_{00}(C_{11}^0 \epsilon_-' - C_{12}^0\, \epsilon_-'') \\ \mathscr{C}^{\mathrm{T}}(z_s^+)\; \mathscr{J}_{00}(C_{21}^0 \epsilon_-' - C_{22}^0\, \epsilon_-'') \\ \mathscr{C}^{\mathrm{T}}(z_s^+)\; \mathscr{J}_{00}(C_{31}^0 \epsilon_-' - C_{32}^0\, \epsilon_-'') \\ \mathscr{C}^{\mathrm{T}}(z_s^+)\; \mathscr{J}_{00}(C_{41}^0 \epsilon_-' - C_{42}^0\, \epsilon_-'') \end{bmatrix} \hat{S}. \tag{3.20}$$

The jth column of ϵ_-', denoted by $(\epsilon_-')_{*j}$, can be expressed in terms of the second column of $C(z_s^-)$:

$$(\epsilon_-')_{*_j} = M^j [C(z_s^-)]_{*2} \tag{3.21a}$$

and also:

$$(\epsilon_-'')_{*_j} = M^j [C(z_s^-)]_{*1} \tag{3.21b}$$

with M^j ($j = 1, 4$), being four (6×4) matrices, which are given in Appendix D.

According to (3.18) the above columns can also be written in terms of the columns of $C(z_0)$:

$$(\epsilon'_-)_{*j} = M^j P(z_s, z_0)\,[C(z_0)]_{*2} \tag{3.22a}$$

and:

$$(\epsilon''_-)_{*j} = M^j P(z_s, z_0)\,[C(z_0)]_{*1}. \tag{3.22b}$$

Substitution of (3.22a) and (3.22b) into (3.20) yields:

$$\hat{B}(z_0) \triangleq \Psi(z_0, z_s^-)\,\hat{S} \triangleq -\frac{[\Delta_{ij}(z_0, z_s^-)]}{\Delta}\,\hat{S} \tag{3.23}$$

with:

$$\Delta_{ij}(z_0, z_s^-) = \mathscr{C}^{\mathrm{T}}(z_s^+)\;\mathscr{I}_{00}\,[\![C^0_{i1} M^j P(z_s, z_0)\,[C(z_0)]_{*2} - C^0_{i2} M^j P(z_s, z_0)\,[C(z_0)]_{*1}]\!]. \tag{3.24}$$

Further, from Appendix D it is easily verified that:

$$C^0_{i1}\,[C(z_0)]_{*2} - C^0_{i2}\,[C(z_0)]_{*1} = (M^i)^{\mathrm{T}}\,\mathscr{C}(z_0) \tag{3.25}$$

with $\mathscr{C}(z_0)$ being the compound vector of $C(z_0)$.

Combining (3.25) with (3.24) yields for $\Delta_{ij}(z_0, z_s^-)$:

$$\Delta_{ij}(z_0, z_s^-) = \mathscr{C}^{\mathrm{T}}(z_s^+)\;\mathscr{I}_{00}(M^j)\,P(z_s, z_0)\,(M^i)^{\mathrm{T}}\;\mathscr{C}(z_0). \tag{3.26}$$

Rewritten in terms of $\mathscr{C}(z_1)$ and $\mathscr{C}(z_2)$ this becomes:

$$\Delta_{ij}(z_0, z_s^-) = \mathscr{C}^{\mathrm{T}}(z_2)\;\mathscr{I}_{00}\;\mathscr{P}(z_2, z_s)\,(M^j)\,P(z_s, z_0)\,(M^i)^{\mathrm{T}}\;\mathscr{P}(z_0, z_1)\;\mathscr{C}(z_1). \tag{3.27}$$

Equation (3.27) allows us to calculate the Ψ-matrix and consequently to compute $\hat{B}(z_0)$ according to (3.23). In the case that the observer point is located in the upper half-space ($z_0 < z_1$) we first calculate $\hat{B}(z_1)$ from:

$$\hat{B}(z_1) = \Psi(z_1, z_s^-)\,\hat{S}$$

and then use the propagator matrix $P_\uparrow(z_0, z_1)$, containing only upgoing waves (Appendix B), to find:

$$\hat{B}(z_0) = P_\uparrow(z_0, z_1)\,\Psi(z_1, z_s^-)\,\hat{S}. \tag{3.28}$$

The above reasoning can be repeated for $z_s < z_0 \leqslant z_2$. Then we obtain:

$$\hat{B}(z_0) \triangleq \Psi(z_0, z_s^+)\,\hat{S} \triangleq +\frac{[\Delta_{ij}(z_0, z_s^+)]}{\Delta}\,\hat{S} \tag{3.29}$$

with:

$$\Delta_{ij}(z_0, z_s^+) = \mathscr{C}^{\mathrm{T}}(z_1)\;\mathscr{I}_{00}\;\mathscr{P}(z_1, z_s)\,(M^j)\,P(z_s, z_0)\,(M^i)^{\mathrm{T}}\;\mathscr{P}(z_0, z_2)\;\mathscr{C}(z_2). \tag{3.30}$$

For the observer point located in the bottom half-space ($z_0 > z_2$) we find:

$$\hat{B}(z_0) = P_\downarrow(z_0, z_2)\,\Psi(z_2, z_s^+)\,\hat{S}, \tag{3.31}$$

wherein $P_\downarrow(z_0, z_2)$ is the propagator matrix containing only downgoing waves.

For the *SH*-waves we obtain similar results. The expressions (3.23), (3.28) and (3.29), (3.31) remain valid but the determinants Δ_{ij} now turn out to be, for $z_1 \leqslant z_0 < z_s$:

$$\Delta_{ij}(z_0, z_s^-) = C^{\mathrm{T}}(z_2)\ \mathscr{J}_{00}\, P(z_2, z_s)\,(N^j)\,(N^i)^{\mathrm{T}}\, P(z_0, z_1)\, C(z_1), \tag{3.32}$$

and for $z_s < z_0 \leqslant z_2$:

$$\Delta_{ij}(z_0, z_s^+) = C^{\mathrm{T}}(z_1)\ \mathscr{J}_{00} P(z_1, z_s)\,(N^j)\,(N^i)^{\mathrm{T}}\, P(z_0, z_2)\, C(z_2). \tag{3.33}$$

Herein are (N^j), $(j = 1, 2)$, two (2×1)-dimensional matrices, given in Appendix D.

In order to find the Green's function $B(x_0, z_0, t)$ at an arbitrary point (x_0, z_0) due to a line source located in the point (x_s, z_s), one has to substitute the appropriate expression for $\hat{B}(z_0)$ into the inverse Fourier integral (2.5) and integrate it along a properly chosen path in the complex wavenumber plane. Let us now investigate the behaviour of the integrand for $k \to \infty$ $[k > \max(k_{Sl})]$. Then γ_{Sl} and γ_{Pl} $(l = 0,\ n+1)$, are all imaginary with positive imaginary part. From the explicit expression of the compound matrix $\mathscr{P}(z, z')$ in Appendix C, one can see that like exponentials, such as $\exp[\pm j2\gamma_S(z-z')]$ or $\exp[\pm j2\gamma_P(z-z')]$ do not occur. The dominant exponential factor is $\exp[-j(\gamma_S + \gamma_P)(z-z')]$, $(z > z')$. For the propagator matrix this is $\exp[-j\gamma_P(z-z')]$.

First consider the case for which $z_1 \leqslant z_0 < z_s$. From (3.27) and (3.11) it follows that the dominant exponential factors are (for homogeneous space):

$$\Delta_{ij} \sim \exp[-j(\gamma_S + \gamma_P)(z_2 - z_s)] \cdot \exp[-j\gamma_P(z_s - z_0)] \cdot \exp[-j(\gamma_S + \gamma_P)(z_0 - z_1)]$$

$$\Delta \sim \exp[-j(\gamma_S + \gamma_P)(z_2 - z_s)] \cdot \exp[-j(\gamma_S + \gamma_P)(z_s - z_0)] \cdot \exp[-j(\gamma_S + \gamma_P)(z_0 - z_1)]. \tag{3.34}$$

Thus $\Psi(z_0, z_s^-)$ behaves like:

$$\Psi(z_0, z_s^-) \sim \exp[+j\gamma_S(z_s - z_0)] \tag{3.35}$$

which is a decaying exponential.

The same reasoning can be applied if different layers are present. The exponents are then sums of these terms over all the layers involved.

If the observer point is located in the upper half-space, an additional decaying exponential appears, coming from the upward propagator matrix $P_\uparrow(z_0, z_1)$.

In the cases for which $z_s < z_0 \leqslant z_2$ or z_0 is located in the bottom half-space, a similar decaying behaviour is found. So, if we *a priori* divide out the dominant exponential factors in Δ_{ij} and Δ, machine overflow can never occur.

Therefore, and because the $\mathscr{P}(z, z')$ matrices are calculated directly from the analytic expressions, precision problems are largely eliminated.

For *SH*-waves dominant factors can also be divided out, yielding similar asymptotic expressions as for *P–SV*-waves.

4 The integration of the inverse Fourier integral

In order to obtain the displacement-stress field $B(x_0, z_0, t)$, in an observer point (x_0, z_0), it is necessary to integrate the inverse Fourier integral (2.5). An investigation of the integrand $\hat{B}(k, z, f)$ reveals a number of singularities in the complex k-plane, for a given (real) frequency. Branch points are introduced by each semi-infinite space through the complex roots:

$$\gamma_{So} = (k_{So}^2 - k^2)^{1/2}; \quad \gamma_{Po} = (k_{Po}^2 - k^2)^{1/2}$$

$$\gamma_{Sn+1} = (k_{Sn+1}^2 - k^2)^{1/2}; \quad \gamma_{Pn+1} = (k_{Pn+1}^2 - k^2)^{1/2}. \tag{4.1}$$

The branch lines plotting convention is taken from Marcuvitz & Felsen (1973, p. 466), and run into the first and third quadrants along the paths $\mathrm{Im}(\gamma)=0$. Furthermore, surface wave poles k_p are situated symmetrically on the real axis (loss-free materials), so that:

$$|k_a| < |k_p| < |k_b|$$

with:

$$k_a \triangleq \max(k_{So}, k_{Sn+1})$$

$$k_b \triangleq \max_i (k_{Si}) \qquad i = 0, 1, \ldots, n+1 \tag{4.2}$$

provided that the stack of layers is terminated on both ends with a semi-infinite space. The complex wavenumber plane situation is shown in Fig. 2 for a one-layer medium sandwiched between two semi-infinite spaces, in the *SH*-case. The path of integration follows the real k-axis, obeying the radiation condition by remaining in the even quadrants. The selected path for the numerical integration is shown in Fig. 3. This path avoids guided mode poles and half-space branch points. These singularities make the main contribution to the integral at very large distances from the source. Because the integrand $\hat{B}(k, z_0, f)$ can be decomposed into even and odd parts, the path can start at the origin. The evaluation of a subintegral over a straight line is done using a Romberg extrapolation scheme combined with a Filon quadrature. From k_4 onwards an asymptotic estimation for the remainder of the integral is made. The choice of the constants $k_1, \ldots k_4$ is done by trial and error to maximize speed. Their values are not critical, except for large $k|x_0-x_s|$ due to the factor $\exp(+jk|x_0-x_s|)$. Therefore, one has to be careful not to move too far in the fourth quadrant so as to avoid a loss of precision in summing the subintegrals. On the other hand coming too close to the poles on the real axis causes also a loss of precision in integrating the subintegrals. One is forced to a compromise which sets a limit on $k|x_0-x_s|$ for a given computation effort.

Other authors (e.g. Kennett 1980) make the medium weakly attenuative so as to shift the singularities from the real axis in the first quadrant. The integration is then performed

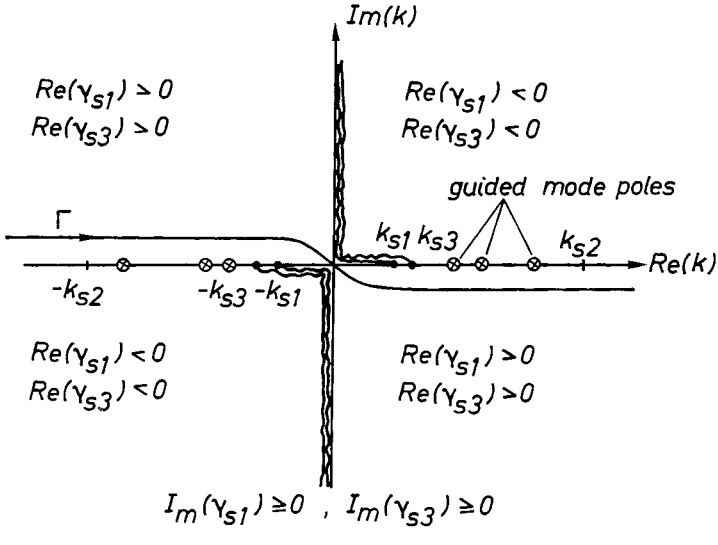

Figure 2. The complex wavenumber plane, showing the upper Riemann sheet. Branch lines and poles are showed for the *SH* case only.

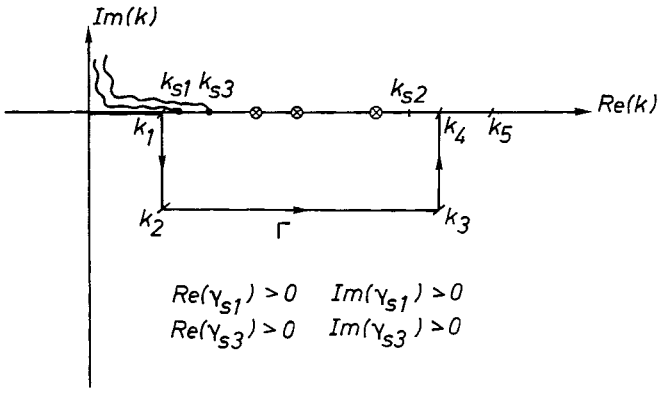

Figure 3. The integration path Γ used in the numerical evaluation of the inverse Fourier integral. Parameters $k_1, \ldots, k_4$ are chosen to maximize speed.

entirely on the real axis. The effect of this attenuation on the resulting pulse forms also sets a limit on $k|x_0 - x_s|$.

While performing the k-integrations for each frequency, the $S_i(f)$ functions ($i = 1, 3$), in (2.7) are kept constant. The spectrum so obtained is the frequency response of the medium for the given source and observer positions. This response is then multiplicated with the spectrum of the source. The frequency to time inversion of this product is then done, using a Fast Fourier Transform routine, to yield the source time response.

5 Numerical results

Two example cases are considered for which time domain solutions are presented. The first one is a theoretical *SH* seismogram for the simple model of the Borrego mountain earthquake event, also used by Heaton & Helmberger (1977), Swanger & Boore (1978) and Kamel & Felsen (1981). This model, which is shown in Fig. 4, consists of a sediment layer of 2.9 km thickness covering a bedrock bulk. The source S is located 9 km below the Earth's surface and horizontally spaced over 60 km from the geophone G. The elastic parameters are indicated in the picture. A triangular source time function is applied:

$$\begin{aligned} S_2(t) &= 2t && 0 \leqslant t < 0.5 \text{ s} \\ &= 2(1-t) && 0.5 \leqslant t < 1 \text{ s} \\ &= 0 && t \geqslant 1 \text{ s} \end{aligned} \tag{5.1a}$$

In Fig. 5 the synthesized time response $u_2(t)$ is shown. It is in good agreement with the

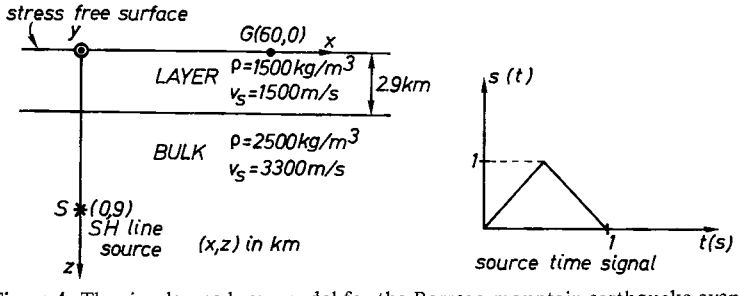

Figure 4. The simple one-layer model for the Borrego mountain earthquake event.

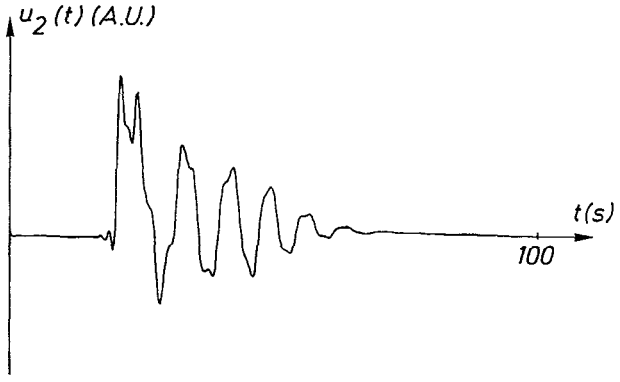

Figure 5. The theoretical *SH* seismogram for the medium of Fig. 4.

result of Kamel & Felsen (1981) who calculated the same seismogram using a hybrid formulation, i.e. a mixed expansion in terms of mode fields and ray integrals. Minor deviations in the detail of the pulse form might be due to a difference in sample rate.

The second medium consists of two layers covering a semi-infinite space as shown in Fig. 6. The surface layer has a thickness of 100 m, followed by a coal layer of 27 m. The source is placed 70 m below the free surface. Three groups of equally spaced geophones are arranged as follows: group A ($G_1 - G_{10}$) is located at the surface with the geophones at 10 m intervals, group B ($G_{11} - G_{22}$) is situated in a borehole 110 m apart from the source, and the group C geophones ($G_{23} - G_{32}$) are also placed at 10 m intervals on a horizontal line 165 m

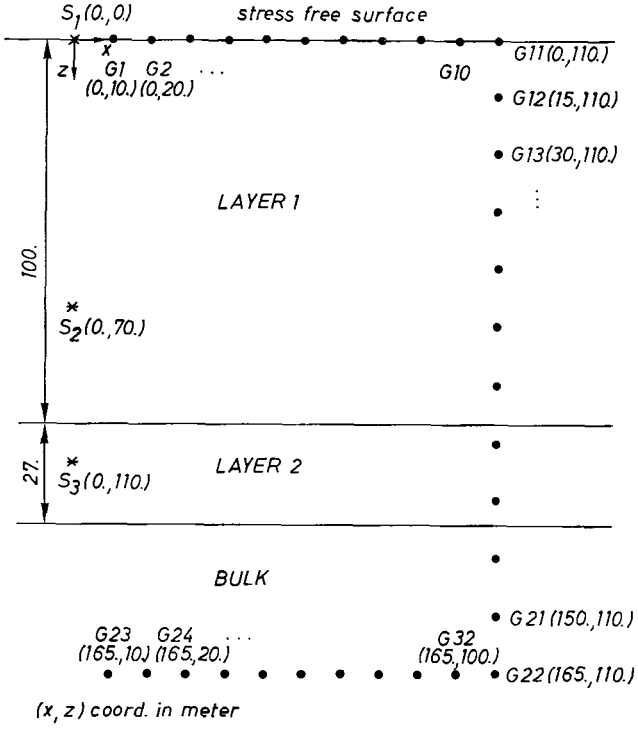

Figure 6. A test medium consisting of two layers on top of a semi-infinite space. The uppermost layer stretches out to the free surface.

below the surface. Time domain displacement functions are calculated for both *SH*- and *P–SV*-wave types. A source time function, called a RICKER wavelet, is used for each source component:

$$s_i(t) = \left(-\frac{F_0}{2}\right)\left[\left(\frac{tF_0}{2}\right)^2 - \frac{1}{2}\right]\exp\left[1-\left(\frac{tF_0}{2}\right)^2\right] \tag{5.1b}$$

The frequency range is limited to 0–200 Hz. The centre frequency F_0 is chosen to be 60 Hz. The elastic parameters for each layer are given in Table 1.

Fig. 7 shows the $u_2(t)$ displacements for the three geophone groups. A number of prominent arrivals can be identified using a planewave ray approximation. Pulses are numbered in order of arrival. In geophone group A, SH_1 marks the direct wavefront from the source S to the surface. Subsequent arrivals are due to reflections on the coal–layer interfaces. In group B, SH_2 is the reflection from the free surface. So is the SH_2 arrival in

Table 1. Elastic data for the two layer example of Fig. 6.

Material	ρ (kg m^{-3})	v_S (m s^{-1})	v_P (m s^{-1})	Thickness (m)
Mat 1	2400	1113	2377	100
Coal	2000	955	2042	27
Mat 2	2400	1173	2499	∞

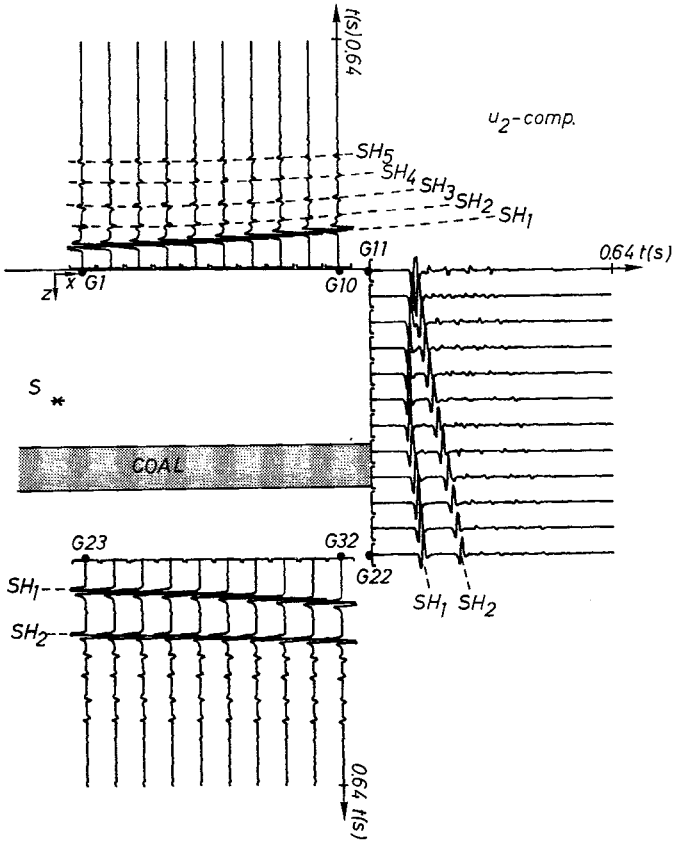

Figure 7. The $u_2(t)$ displacements for the medium of Fig. 6.

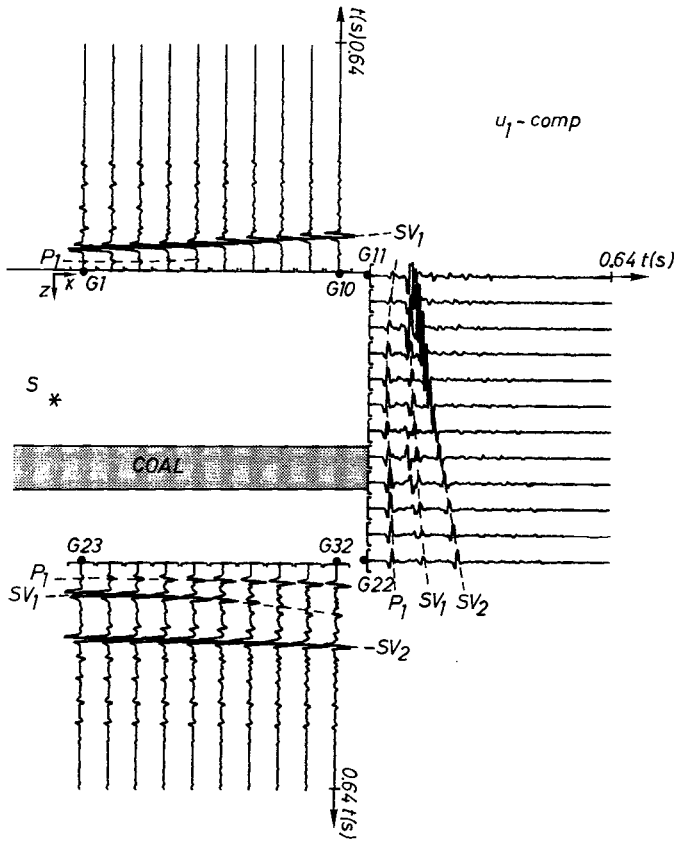

Figure 8. The $u_1(t)$ displacements for the medium of Fig. 6.

group C. In Fig. 8 the $u_1(t)$ displacements are shown. In group A the first arrival is the projection on the x-axis of the displacement vector of the compressional wave (P_1), travelling at the velocity v_P of the upper layer to the surface. At the same arrival time, its projection on the z-axis can be seen in Fig. 9, showing the $u_3(t)$ displacement component. The strong response, marked with SV_1 in both figures, is the direct shear arrival. In the B group, from Figs 8 and 9, one can see the direct P_1 and SV_1 wavefronts. The response marked with SV_2 is the shear reflection at the free surface. Those three arrivals are also present in the C group. More pulses can be identified by taking the multiple reflections into account on the coal–layer interfaces. A complete analysis of these seismograms, however, is beyond the topic of this paper. Previous examples show that the proposed method works well and is free of any numerical problems.

The classical propagator matrix method, as noted earlier, cannot be used to calculate P–SV solutions for high frequencies due to its sensitivity to round-off errors. This numerical problem causes a limit to the thickness of the stack of layers for which acceptable results can be achieved, for a given finite accuracy computation. Beyond that limit, no results can be obtained unless the number of digits used in the computations is enlarged. This obviously increases the CPU time needed to solve the problem. To obtain a reliable estimation for this limit, the following test has been made. For a symmetric one-layer waveguide, the boundary system determinant is calculated, in the P–SV case, from equation (3.11), ($z_s = z_2$):

$$\Delta_C = \mathscr{C}_2^{\mathrm{T}} \; \mathscr{I}_{00} \; \mathscr{P}(z_2, z_1) \; \mathscr{C}_1. \tag{5.2}$$

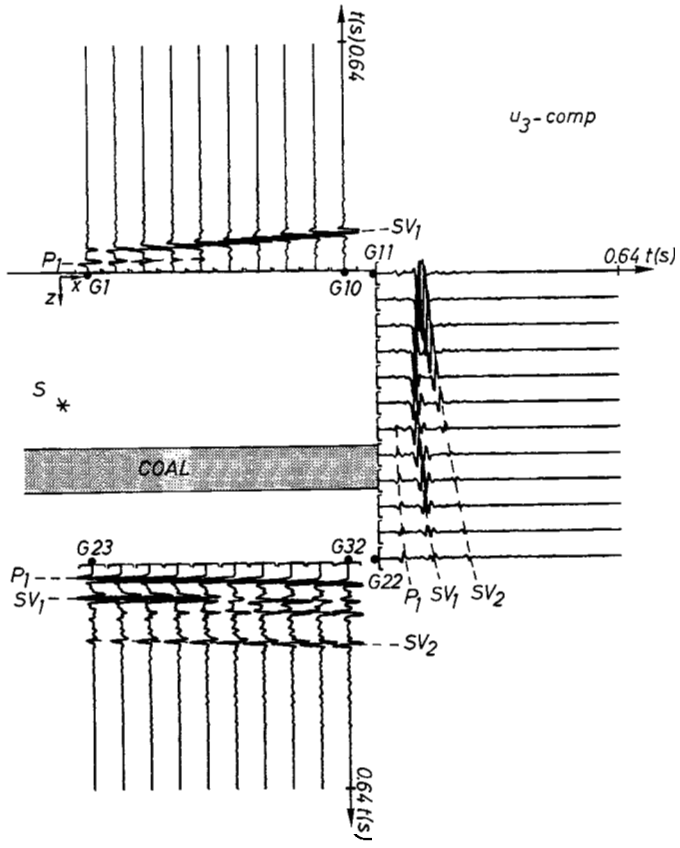

Figure 9. The $u_3(t)$ displacements for the medium of Fig. 6.

This result is compared with the value which could be obtained by the propagator matrix method (equation 3.3):

$$\Delta_P = \det \{[C(z_2) \quad P(z_2, z_1)\, C(z_1)]\}. \tag{5.3}$$

Both determinants were computed using single precision (eight digits) yielding $\Delta_C^{(1)}$ and $\Delta_P^{(1)}$ and double precision (16 digits) yielding $\Delta_C^{(2)}$ and $\Delta_P^{(2)}$. The value $\Delta_C^{(2)}$ was regarded as the reference value. The wavenumber was chosen to be $k = 1.2\ k_S$ (k_S = shear wavenumber in the coal layer). The leading exponential factor:

$$\exp[-j(\gamma_S + \gamma_P)D] \tag{5.4}$$

was omitted to ensure that the determinants remain bounded for $D \to +\infty$.

Fig. 10 shows a plot of the logarithm of the relative error in each case, compared with $\Delta_C^{(2)}$, as a function of D/λ_S. The test medium elastic data are given in Table 2.

With 16 digits precision the propagator matrix method error exceeds the eight digits modified propagator matrix method beyond $D = 8\lambda_S$. At $D = 14\lambda_S$ the relative error in $\Delta_P^{(2)}$ rises already to 100 per cent. Even for $D < 7\lambda_S$ the obtained accuracy of $\Delta_C^{(1)}$ (better than $\mathbf{10^{-6}}$) is only one order of magnitude worse than that of $\Delta_P^{(2)}$. This indicates that even for thin layers the propagator matrix method is much more sensitive to round-off errors than the modified method. Finally, the relative error in $\Delta_P^{(1)}$ exceeds that in $\Delta_C^{(1)}$ already for

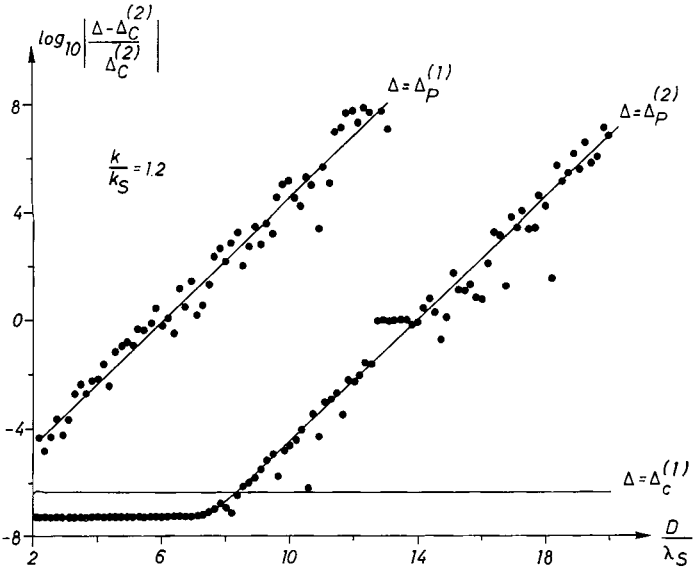

Figure 10. A plot of the logarithm of the relative error in the computation of the boundary system determinant for a one-layer waveguide as a function of the normalized thickness of the layer. The dots represent the error using the traditional propagator matrix method. For the parameters see text.

Table 2. The elastic data for the test medium which was used to produce Fig. 6.

Material	ρ(kg m^{-3})	v_S(m s^{-1})	v_P(m s^{-1})	Thickness (m)
Stone	2460	2340	4230	∞
Coal	1364	1140	2370	D (variable)
Stone	2460	2340	4230	∞

$D = \lambda_S$, showing that single precision calculations cannot be used for the classical propagator matrix method. We can conclude that is is not necessary to use more than eight digits precision for the computation of the Green's function. In all applications handled with the modified propagator matrix method, five digit accuracy was easily obtained for the displacements. Therefore, memory storage space and run time are substantially reduced by this method. The program package which is used to calculate synthetic seismograms is written in FORTRAN '77 and runs on a VAX 11/750 computer, without a floating point processor. Up to 10 traces are integrated together if the geophone locations have the same depth levels. When this is the case, the integrands differ only in the exponential factor $\exp[jk(x_0-x_s)]$. To produce 10 traces, sampled in the frequency domain in 64 points, it takes an amount of CPU time as shown in Table 3, depending on the number of layers.

Table 3. Consumed CPU time as a function of the number of layers.

Number of layers	*SH* case	*P–SV* case (hr)
1	20 min	2
4	1.5 hr	7
8	2 hr	12.5

6 Conclusions

It has been shown that the numerical difficulties, inherent in the classical propagator matrix approach of Thomson-Haskell, can be avoided without losing the practical matrix formulation of that method. Using a mixture of propagator matrices and compound propagator matrices, the integrand of the inverse Fourier integral can be calculated for any layer thickness. It has also been shown that the modified method is much less sensitive to round-off errors than the original formulation and therefore can run in single (eight digits) precision. The somewhat larger computational effort required in machine storage and computing time for the integrand can be neglected, compared with the gain in precision and the resulting enhancement of the integration convergence.

The general idea outlined in this paper could, in theory, also be used to calculate the elasto-dynamic Green's function in anisotropic media. To that end, one has to derive the appropriate analytical expressions for the propagator matrix and the compound matrix. However, this might not be a trivial task.

Finally, we mention that the choice of a source should not be restricted to a single force excitation, as used in (2.1). Any combined force system, including the source moment tensor (Gilbert 1971), can be used. The result will be a more complex jump vector $\hat{S}$ in (2.23) in which the displacements (in the k-domain) will, in general, be discontinuous across the $z = z_s$ plane.

Acknowledgments

The author wishes to thank Professor P. E. Lagasse for his helpful discussions and remarks. He also would like to thank IWONL for a grant.

References

Abo-Zena, A., 1979. Dispersion function computations for unlimited frequency values, *Geophys. J. R. astr. Soc.*, **58**, 91–105.

Aki, K. & Richards, P. L., 1980. *Quantitative Seismology – Theory and Methods,* Freeman, San Francisco.

Dunkin, J. W., 1965. Computations of modal solutions in layered elastic media at high frequencies, *Bull. seism. Soc. Am.*, **55**, 335–358.

Gantmacher, F. R., 1959. *The Theory of Matrices, 1,* Chelsea, New York.

Gilbert, F., 1971. The excitation of the normal modes of the Earth by earthquake sources, *Geophys. J. R. astr. Soc.*, **22**, 223–226.

Gilbert, F. & Backus, G. E., 1965. Propagator matrices in elastic waves and vibration problems, *Geophysics,* **31**, 326–332.

Harkrider, D. G., 1964. Surface waves in multilayered elastic media I. Rayleigh and Love waves from buried sources in a multilayered elastic half-space, *Bull. seism. Soc. Am.*, **54**, 627–679.

Haskell, N. A., 1953. The dispersion of surface waves on multilayered media, *Bull. seism. Soc. Am.*, **43**, 17–34.

Haskell, N. A., 1964. Radiation pattern of surface waves from point sources in a multilayered medium, *Bull. seism. Soc. Am.*, **54**, 377–393.

Heaton, T. H. & Helmberger, D. V., 1977. A study of strong ground motion of the Borrego Mountain, California, earthquake, *Bull. seism. Soc. Am.*, **67**, 315–330.

Kamel, A. & Felsen, L. B., 1981. Hybrid ray-mode formulation of *SH* motion in a two layer half space, *Bull. seism. Soc. Am.*, **71**, 1763–1781.

Kennett, B. L. N., 1980. Seismic waves in a stratified half-space – II. Theoretical seismograms, *Geophys. J. R. astr. Soc.*, **61**, 1–10.

Kennett, B. L. N. & Kerry, N. J., 1979. Seismic waves in a stratified half-space, *Geophys. J. R. astr. Soc.*, **57**, 557–583.

Kennett, B. L. N., Kerry, N. J. & Woodhouse, J. H., 1978. Symmetries in the reflection and transmissions of elastic waves, *Geophys. J. R. astr. Soc.*, **52**, 215–230.

Knopoff, L., 1964. A matrix method for elastic waves problems, *Bull. seism. Soc. Am.*, **54**, 431–438.
Marcuvitz, N. & Felsen, L. B., 1973. *Radiation and Scattering of Waves*, Prentice Hall, New York.
Molotkov, L. A., 1961. On the propagation of elastic waves in media consisting of thin plane parallel layers, problems in the theory of seismic wave propagation, *Nank. Leningr.*, 240–281 (in Russian).
Swanger, H. J. & Boore, D. M., 1978. Simulation of strong motion displacement using surface wave modal superposition, *Bull. seism. Soc. Am.*, **68**, 907–922.
Thomson, W. T., 1950. Transmission of elastic waves through a stratified medium, *J. appl. Phys.*, **21**, 89–93.
Woodhouse, J. H., 1981. Efficient and stable methods for performing seismic calculations in stratified media, *Physics of the Earth's Interior*, eds Dziewonski, A. M. & Boschi, E., Elsevier, New York.

Appendix A

Let us denote by:

μ, λ: the Lamé constants for an isotropic layer,
ρ: the volume density of a material,
$\omega = 2\pi f$: the harmonic pulsation,
j: the imaginary unit,
$v_S = \sqrt{\mu/\rho}$: shear phase velocity,
$v_P = \sqrt{(\lambda + 2\mu)/\rho}$: compressional phase velocity,
$k_S = \omega/v_S$: shear wavenumber,
$k_P = \omega/v_P$: compressional wavenumber,
$\gamma_S = (k_S^2 - k^2)^{1/2}$: transverse shear wavenumber,
$\gamma_P = (k_P^2 - k^2)^{1/2}$: transverse compressional wavenumber with the assumption:

$$\mathrm{Re}(\gamma_S) \geqslant 0, \qquad \mathrm{Im}(\gamma_S) \geqslant 0$$

$$\mathrm{Re}(\gamma_P) \geqslant 0, \qquad \mathrm{Im}(\gamma_P) \geqslant 0.$$

The (2×2) system matrix A in (2.6) for *SH*-waves is then given by:

$$A = \begin{bmatrix} 0 & \mu^{-1} \\ -\mu\gamma_S^2 & 0 \end{bmatrix} \tag{A1}$$

while for *P–SV*-waves, A is the (4×4) matrix:

$$A = \begin{bmatrix} 0 & -jk & \mu^{-1} & 0 \\ -jk\eta & 0 & 0 & \mu^{-1}\epsilon \\ \mu[4(\epsilon+\eta)k^2 - k_S^2] & 0 & 0 & -jk\eta \\ 0 & -\mu k_S^2 & -jk & 0 \end{bmatrix} \tag{A2}$$

with:

$\epsilon = \mu/(\lambda + 2\mu) \qquad \eta = \lambda/(\lambda + 2\mu).$

Let us further denote by D the matrix of eigenvectors of the system matrix A and by Λ the diagonal matrix of eigenvalues of A. So:

$$A = D\Lambda D^{-1}. \tag{A3}$$

Then, in the *SH* case, we obtain for:

$$\Lambda = \mathrm{diag}\ \{-j\gamma_S, +j\gamma_S\} \tag{A4}$$

while the eigenvector matrix can be chosen to be:

$$D = \frac{1}{\sqrt{2}} \begin{bmatrix} 1 & 1 \\ -j\mu\gamma_S & +j\mu\gamma_S \end{bmatrix} \tag{A5}$$

with its inverse:

$$D^{-1} = \frac{1}{\sqrt{2}} \begin{bmatrix} 1 & j\mu^{-1}\gamma_S^{-1} \\ 1 & -j\mu^{-1}\gamma_S^{-1} \end{bmatrix} . \tag{A6}$$

In the P–SV case, Λ is given by:

$$\Lambda = \text{diag}\,\{-j\gamma_S, -j\gamma_P, +j\gamma_S, +j\gamma_P\} . \tag{A7}$$

The eigenvector matrix can be chosen to be:

$$D = \frac{1}{\sqrt{2}} \begin{bmatrix} -j\gamma_S & jk & j\gamma_S & jk \\ -jk & -j\gamma_P & -jk & j\gamma_P \\ \mu(2k^2-k_S^2) & 2\mu k\gamma_P & \mu(2k^2-k_S^2) & -2\mu k\gamma_P \\ -2\mu k\gamma_S & \mu(2k^2-k_S^2) & 2\mu k\gamma_S & \mu(2k^2-k_S^2) \end{bmatrix} \tag{A8}$$

with its inverse:

$$D^{-1} = \frac{1}{\sqrt{2}\mu k_S^2} \begin{bmatrix} -j\mu\gamma_S^{-1}(2k^2-k_S^2) & j2\mu k & -1 & -k\gamma_S^{-1} \\ -j2\mu k & -j\mu\gamma_P^{-1}(2k^2-k_S^2) & k\gamma_P^{-1} & -1 \\ j\mu\gamma_S^{-1}(2k^2-k_S^2) & j2\mu k & -1 & k\gamma_S^{-1} \\ -j2\mu k & j\mu\gamma_P^{-1}(2k^2-k_S^2) & -k\gamma_P^{-1} & -1 \end{bmatrix} . \tag{A9}$$

Appendix B

The propagator matrix $P(z, z')$ satisfies the homogeneous system:

$$\partial_z P(z, z') = A\,P(z, z'). \tag{B1}$$

Using the transformation (2.10), one finds that the propagator matrix is given by:

$$P(z, z') = D \exp[\Lambda(z-z')]\, D^{-1}. \tag{B2}$$

Let d_{ij} be the ijth element of D and δ_{ij} the ijth element of D^{-1}. $P(z, z')$ can then also be written as follows:

For SH-waves:

$$P(z, z') = P^- \exp[-j\gamma_S(z-z')] + P^+ \exp[+j\gamma_S(z-z')] \tag{B3a}$$

with:

$$\begin{aligned} P_{ij}^- &= d_{i1}\,\delta_{1j} \\ P_{ij}^+ &= d_{i2}\,\delta_{2j}. \end{aligned} \qquad (i, j = 1, 2) \tag{B3b}$$

For P–SV-waves:

$$P(z, z') = P^- \exp[-j\gamma_S(z-z')] + P^+ \exp[+j\gamma_S(z-z')] + Q^- \exp[-j\gamma_P(z-z')] + Q^+ \exp[+j\gamma_P(z-z')] \tag{B4a}$$

with:

$$P_{ij}^- = d_{i1}\,\delta_{1j} \qquad Q_{ij}^- = d_{i2}\,\delta_{2j}$$
$$P_{ij}^+ = d_{i3}\,\delta_{3j} \qquad Q_{ij}^+ = d_{i4}\,\delta_{4j} \qquad (i, j = 1, 4)\ . \tag{B4b}$$

For $z > z'$, it is clear, noticing the sign convention of the complex roots γ_S and γ_P, that $P^- \exp[-j\gamma_S(z-z')]$ becomes the leading term in the evanescent regime for SH-waves, whereas $Q^- \exp[-j\gamma_P(z-z')]$ becomes it in the case of P–SV-waves. Furthermore, it is worth noticing that the rank of the coefficient matrices in (B3b) and (B4b) is 1.

The upward and downward propagators are respectively given by:

SH case:

$$P_\uparrow(z, z') = P^- \exp[-j\gamma_S(z-z')] \tag{B5a}$$

$$P_\downarrow(z, z') = P^+ \exp[+j\gamma_S(z-z')]. \tag{B5b}$$

P–SV case:

$$P_\uparrow(z, z') = P^- \exp[-j\gamma_S(z-z')] + Q^- \exp[-j\gamma_P(z-z')] \tag{B6a}$$

$$P_\downarrow(z, z') = P^+ \exp[+j\gamma_S(z-z')] + Q^+ \exp[+j\gamma_P(z-z')]. \tag{B6b}$$

Appendix C

The compound matrix of the propagator matrix, denoted by $\mathscr{P}(z, z')$, is the (6×6) matrix of second-order minors, arranged in the way:

$$\mathscr{P}(z, z') = \begin{bmatrix} \binom{12}{12} & \binom{12}{13} & \binom{12}{14} & \binom{12}{23} & \binom{12}{24} & \binom{12}{34} \\ \binom{13}{12} & \binom{13}{13} & \cdots & & & \\ \vdots & \vdots & & & & \\ \binom{34}{12} & & \cdots & & & \binom{34}{34} \end{bmatrix}. \tag{C1}$$

This matrix can be calculated directly from (B2) by replacing these matrices with their compound versions:

$$\mathscr{P}(z, z) = \mathscr{D} \exp[\mathscr{A}(z-z')]\, \mathscr{D}^{-1}. \tag{C2}$$

Herein are $\mathscr{D}$ and $\mathscr{D}^{-1}$ the (6×6) compound matrices of the eigenmatrix D and its inverse D^{-1} respectively. The diagonal matrix $\exp[\mathscr{A}(z-z')]$ is given by:

$$\exp[\mathscr{A}(z-z')] = \exp[\mathrm{diag}\,\{-j(\gamma_S+\gamma_P)(z-z'), 0, -j(\gamma_S-\gamma_P)(z-z'), +j(\gamma_S-\gamma_P)(z-z'), 0, +j(\gamma_S+\gamma_P)(z-z')\}]. \tag{C3}$$

Written in the form of a linear combination of exponential terms another expression for $\mathscr{P}(z, z')$ is:

$$\mathscr{P}(z, z') = \mathscr{P}^1 \exp[-j(\gamma_S + \gamma_P)(z-z')] + \mathscr{P}^2 + \mathscr{P}^3 \exp[-j(\gamma_S - \gamma_P)(z-z')] + \mathscr{P}^4 \exp[+j(\gamma_S - \gamma_P)(z-z')] + \mathscr{P}^5 + \mathscr{P}^6 \exp[+j(\gamma_S + \gamma_P)(z-z')]. \quad \text{(C4)}$$

The (m, n)th element $\mathscr{P}^r_{mn}$ of each coefficient matrix can be computed directly from the elements of the compound eigenvector matrix and its inverse, as follows:

$$\mathscr{P}^r_{mn} = \mathscr{D}_{mr}\, \mathscr{D}^{-1}_{rn}. \quad \text{(C5)}$$

Define:

$w = k/k_S; g_S = \gamma_S/k_S; g_P = \gamma_P/k_S$

$u = 2w^2 - 1; f_S = g_S^{-1}; f_P = g_P^{-1}$

$g = g_S g_P; f = f_S f_P$

$p = -jk_S; q = \mu k_S^2.$

The $\mathscr{D}$ matrix then consists of the following rows:

$$\mathscr{D}_{1*} = \tfrac{1}{2} p^2 [(g + w^2), 2g_S w, -(g - w^2), (g - w^2), 2g_P w, (g + w^2)]$$

$$\mathscr{D}_{2*} = \tfrac{1}{2} pq [w(2g + u), 2g_S u, -w(2g - u), w(2g - u), 4g_P w^2, w(2g + u)]$$

$$\mathscr{D}_{3*} = \tfrac{1}{2} pq [-g_S, 0, -g_S, -g_S, 0, +g_S]$$

$$\mathscr{D}_{4*} = \tfrac{1}{2} pq [+g_P, 0, -g_P, -g_P, 0, -g_P]$$

$$\mathscr{D}_{5*} = \tfrac{1}{2} pq [w(2g + u), 4g_S w^2, -w(2g - u), w(2g - u), 2g_P u, w(2g + u)]$$

$$\mathscr{D}_{6*} = \tfrac{1}{2} q^2 [(4gw^2 + u^2), 4g_S wu, -(4gw^2 - u^2), (4gw^2 - u^2), 4g_P wu, (4gw^2 + u^2)]. \quad \text{(C6a)}$$

The $\mathscr{D}^{-1}$ matrix consists of the columns:

$$\mathscr{D}^{-1}_{*1} = \tfrac{1}{2} p^{-2} [(fu^2 + 4w^2), -4f_S wu, -(fu^2 - 4w^2), (fu^2 - 4w^2), -4f_P wu, (fu^2 + 4w^2)]^{\mathrm{T}}$$

$$\mathscr{D}^{-1}_{*2} = \tfrac{1}{2} p^{-1} q^{-1} [-w(fu + 2), 2f_S u, w(fu - 2), -w(fu - 2), 4f_P w^2, -w(fu + 2)]^{\mathrm{T}}$$

$$\mathscr{D}^{-1}_{*3} = \tfrac{1}{2} p^{-1} q^{-1} [-f_S, 0, -f_S, -f_S, 0, +f_S]^{\mathrm{T}}$$

$$\mathscr{D}^{-1}_{*4} = \tfrac{1}{2} p^{-1} q^{-1} [+f_P, 0, -f_P, -f_P, 0, -f_P]^{\mathrm{T}} \quad \text{(C6b)}$$

$$\mathscr{D}^{-1}_{*5} = \tfrac{1}{2} p^{-1} q^{-1} [-w(fu + 2), 4f_S w^2, w(fu - 2), -w(fu - 2), 2f_P u, -w(fu + 2)]^{\mathrm{T}}$$

$$\mathscr{D}^{-1}_{*6} = \tfrac{1}{2} q^{-2} [(fw^2 + 1), -2f_S w, -(fw^2 - 1), (fw^2 - 1), -2f_P w, (fw^2 + 1)]^{\mathrm{T}}.$$

Appendix D

The four matrices M^j, $(j = 1, 4)$, are given by:

$$M^1 = \begin{bmatrix} 0 & 1 & 0 & 0 \\ 0 & 0 & 1 & 0 \\ 0 & 0 & 0 & 1 \\ 0 & 0 & 0 & 0 \\ 0 & 0 & 0 & 0 \\ 0 & 0 & 0 & 0 \end{bmatrix} \qquad M^2 = \begin{bmatrix} -1 & 0 & 0 & 0 \\ 0 & 0 & 0 & 0 \\ 0 & 0 & 0 & 0 \\ 0 & 0 & 1 & 0 \\ 0 & 0 & 0 & 1 \\ 0 & 0 & 0 & 0 \end{bmatrix} \quad \text{(D1a, b)}$$

$$M^3 = \begin{bmatrix} 0 & 0 & 0 & 0 \\ -1 & 0 & 0 & 0 \\ 0 & 0 & 0 & 0 \\ 0 & -1 & 0 & 0 \\ 0 & 0 & 0 & 0 \\ 0 & 0 & 0 & 1 \end{bmatrix} \qquad M^4 = \begin{bmatrix} 0 & 0 & 0 & 0 \\ 0 & 0 & 0 & 0 \\ -1 & 0 & 0 & 0 \\ 0 & 0 & 0 & 0 \\ 0 & -1 & 0 & 0 \\ 0 & 0 & -1 & 0 \end{bmatrix} . \qquad \text{(D1c, d)}$$

For *SH*-waves, the N^j, $(j = 1, 2)$, are:

$$N^1 = \begin{bmatrix} 1 \\ 0 \end{bmatrix} \qquad N^2 = \begin{bmatrix} 0 \\ 1 \end{bmatrix} . \qquad \text{(D2a, b)}$$